J. Mol. Biol. (1992) 224, 487–499

Antibody Framework Residues Affecting the Conformation of the Hypervariable Loops

Jefferson Foote and Greg Winter

MRC Laboratory of Molecular Biology
Hills Road, Cambridge CB2 2QH, England

(Received 17 September 1991; accepted 25 November 1991)

Rodent monoclonal antibodies have been "humanized" or "reshaped" for therapy by transplanting the antigen-binding loops from their variable domains onto the β-sheet framework regions of human antibodies. However, additional substitutions in the human framework regions are sometimes required for high affinity antigen binding. Here we describe antigen binding by a reshaped antibody derived from the mouse anti-lysozyme antibody D1.3, and several variants in which point mutations had been introduced into framework positions to improve its affinity. The affinities were determined from the relaxation kinetics of reactant mixtures using quenching of fluorescence that occurs upon formation of the antibody–antigen complex. The dissociation constant of lysozyme ranged from 3·7 nM (for D1.3) to 260 nM. Measurement of antibody–antigen association kinetics using stopped-flow showed that D1.3 and most of the reshaped antibodies had bimolecular rate constants of $1{\cdot}4 \times 10^6$ s^{-1} M^{-1}, indicating that differences in equilibrium constant were predominantly due to different rates of dissociation of lysozyme from immune complexes. Mutations in a triad of heavy chain residues, 27, 29 and 71, contributed 0·9 kcal/mol in antigen binding free energy, and a Phe to Tyr substitution of light chain residue 71 contributed an additional 0·8 kcal/mol. The combined effect of all these mutations brought the affinity of the reshaped antibody to within a factor of 4 of D1.3. All of these substitutions were in the β-sheet framework closely underlying the complementarity-determining regions, and do not participate in a direct interaction with antigen. The informed selection of residues in such positions may prove essential for the success of loop transplants in antibodies. Variation of these sites may also have a role in shaping the diversity of structures found in the primary repertoire, and in affinity maturation.

Keywords: humanized antibody; kinetics; site-directed mutagenesis; hypervariable loop; lysozyme

1. Introduction

The antibody is a Y-shaped molecule, in which the variable (V) domains forming the tips of the arms bind to antigen and those forming the stem (C-domains) are responsible for triggering effector functions that eliminate antigen. X-ray diffraction studies of crystalline antibody fragments reveal the V and C-domains as two layers of β-pleated sheet, with loops connecting the ends of the β-strands (Poljak *et al.*, 1973; Schiffer *et al.*, 1973; Segal *et al.*, 1974). In the heavy and light chain V-domains the loops at one end of the sheet are hypervariable in sequence (Wu & Kabat, 1970; Kabat & Wu, 1971), and form the antigen-binding site. The β-sheet provides a scaffold for mounting a diversity of loops, and indeed the antigen binding site can be transplanted from a rodent antibody to a human antibody, thereby "humanizing" the rodent antibody, by transplanting these loops (Jones *et al.*, 1986; Verhoeyen *et al.*, 1988; Riechmann *et al.*, 1988). The clinical success of one such "reshaped" human anti-lymphocyte antibody, CAMPATH-1 (Riechmann *et al.*, 1988) in treating B-cell lymphoma (Hale *et al.*, 1988) and vasculitis (Mathieson *et al.*, 1990), has prompted the reshaping of antibodies directed against the interleukin-2 receptor (Queen *et al.*, 1989), CD4 (Gorman *et al.*, 1991) respiratory syncytial virus (Tempest *et al.*, 1991), herpes simplex virus (Co *et al.*, 1991), human immunodeficiency virus (Maeda *et al.*, 1991) and epidermal growth factor receptor (Kettleborough *et al.*, 1991).

However, reshaping requires that the rodent and human framework regions are structurally conserved, both in the orientation of the two β-sheets of each domain and in the packing of the heavy and light chain V-domains together; that the

0022–2836/92/060487–13 $03.00/0

hypervariable loops make the majority of contacts with antigen; and that the loops are supported in a similar way by the underlying β-sheet framework. Although these are likely to be true for some antibodies, the restitution of key contacts between loops and framework has proved necessary in others, and has been assisted by molecular modelling (Riechmann *et al.*, 1988; Tempest *et al.*, 1991) and systematic matching of rodent and human framework regions to minimize differences in primary sequences (Queen *et al.*, 1989; Gorman *et al.*, 1991; Maeda *et al.*, 1991). As a model we have reshaped a human antibody based on the hypervariable regions of mouse antibody D1.3 (Amit *et al.*, 1986; Bhat *et al.*, 1990) and the framework regions of human Vκ(I) family (Kabat *et al.*, 1987) and the myeloma protein NEW (Poljak *et al.*, 1973). The parent antibody structures have all been solved crystallographically. The Bence–Jones protein REI is in the Vκ(I) family (Epp *et al.*, 1974), and the D1.3 antibody was solved alone and in complex with the antigen lysozyme (Amit *et al.*, 1986; Bhat *et al.*, 1990). We achieved large enhancement of antigen affinity by substitution of several framework residues of a group that may exert a determining influence on the conformation of the CDRs†.

2. Antibody Design

The original distinction between hypervariable regions and framework residues (Wu & Kabat, 1970) had its basis in homologies between the primary sequences of immunoglobulins known at that time. However, as X-ray crystallographic structures became available, it became apparent that residues in the hypervariable regions formed the apical loops connecting the β-strands of the immunoglobulin fold, but could also extend part way along the β-strands themselves (Poljak *et al.*, 1973; Schiffer *et al.*, 1973; Segal *et al.*, 1974). Indeed structural analyses have invoked fewer, and in some cases different, residue positions as CDRs (for example, see Chothia & Lesk, 1987). In X-ray crystallographic structures of antigen–antibody complexes, all the CDRs do not necessarily make contact to antigen (Tulip *et al.*, 1989) and in particular the C-terminal portion of VH-CDR2 has never been shown to interact directly with antigen.

We based our designs on Kabat (Kabat *et al.*, 1987). The construction of the reshaped heavy chain has been described (Verhoeyen *et al.*, 1988). The framework amino acid sequences chosen for the light chain CDR acceptor were designed *de novo*. They are a consensus of human κ subgroup I sequences (Kabat *et al.*, 1987) and closely related (but not identical) to the sequence of the myeloma protein REI (Palm & Hilschmann, 1975). The framework sequences of the first reshaped antibody differ from D1.3 at 18 positions in the light chain and 30 in the heavy chain. The location of these residues is shown in the α-carbon traces of the variable domains of the D1.3 structure in Figure 1(a). The differences are dispersed over the entire variable region of the antibody; all eight framework segments have multiple replacements. The most numerous, half of the total, occur in framework 3 (between CDR2 and CDR3) of both the light and heavy chain. As expected, few differences are seen at the VH–Vκ framework interface, as this region is generally conserved. Two-thirds of the framework differences are located on the molecule's surface and are unlikely to affect antigen binding. There are also differences in buried residues, particularly at the interfaces with the hypervariable regions. We considered retaining these buried framework residues from mouse D1.3 in the reshaped antibody (Padlan, 1991), but even buried residues can form the critical element of a T-cell epitope if presented as a denatured peptide by a class II MHC molecule (Allen *et al.*, 1985). This could exacerbate any humoral response to the native antibody, for example an anti-idiotype reaction, and we therefore used the entire human framework regions, whether the residues were buried or not.

To probe the role of specific framework residues in supporting the CDR conformations, we introduced several additional framework substitutions into the reshaped antibody (VL: Phe71 to Tyr; VH Ser27 to Phe, Thr28 Phe29 Ser30 to Ser Leu Thr, and Lys71 to Val; see Fig. 1(b)).

Residue 71 of the light chain lies in a loop connecting β-strands and the tyrosine ring of D1.3 protrudes inward and is sandwiched between this loop and VL-CDR1 loop. The phenolic oxygen appears to be important: it hydrogen-bonds to the amide nitrogen and carbonyl of Gly68 and the backbone amide nitrogen of Asn31, thus forming a bridge between the two loops. The neighbouring residue Tyr32 is in intimate contact with lysozyme residue Gln121, previously identified as a central feature of the D1.3 recognition site (Amit *et al.*, 1986). Residue Phe71 was therefore changed to Tyr.

Residues 27 to 30 of the heavy chain are part of a structural loop which includes VH-CDR1 (Kabat *et al.*, 1987). Indeed they are included within a structure-based hypervariable loop that comprises residues 26 to 32 (Chothia & Lesk, 1987) compared with VH-CDR1 that comprises 31 to 35 (Kabat *et al.*, 1987). These residues appear to make important interactions with CDR1 and CDR2. For example, in the D1.3 structure, Leu29 packs against Phe27 and Lys71 (see below), and Phe27 packs against residues 31 to 34. In turn Gly31 and Tyr32 of VH-CDR1 make contact with Lys16 of lysozyme. Residue Ser27 would be expected to create a cavity, and was therefore changed to Phe as in D1.3 and Riechmann *et al.* (1988). Residues Thr28, Phe 29, Ser30 were changed *en bloc* to Ser, Leu, Thr.

Residue 71 of the heavy chain may fix the relative dispositions of CDR1 and CDR2, according to

† Abbreviations used: CDR, complementarity-determining region; ELISA, enzyme-linked immunosorbent assay; PBS, phosphate-buffered saline; K_{aa}, equilibrium dissociation constant; kb, 10^3 bases or base-pairs.

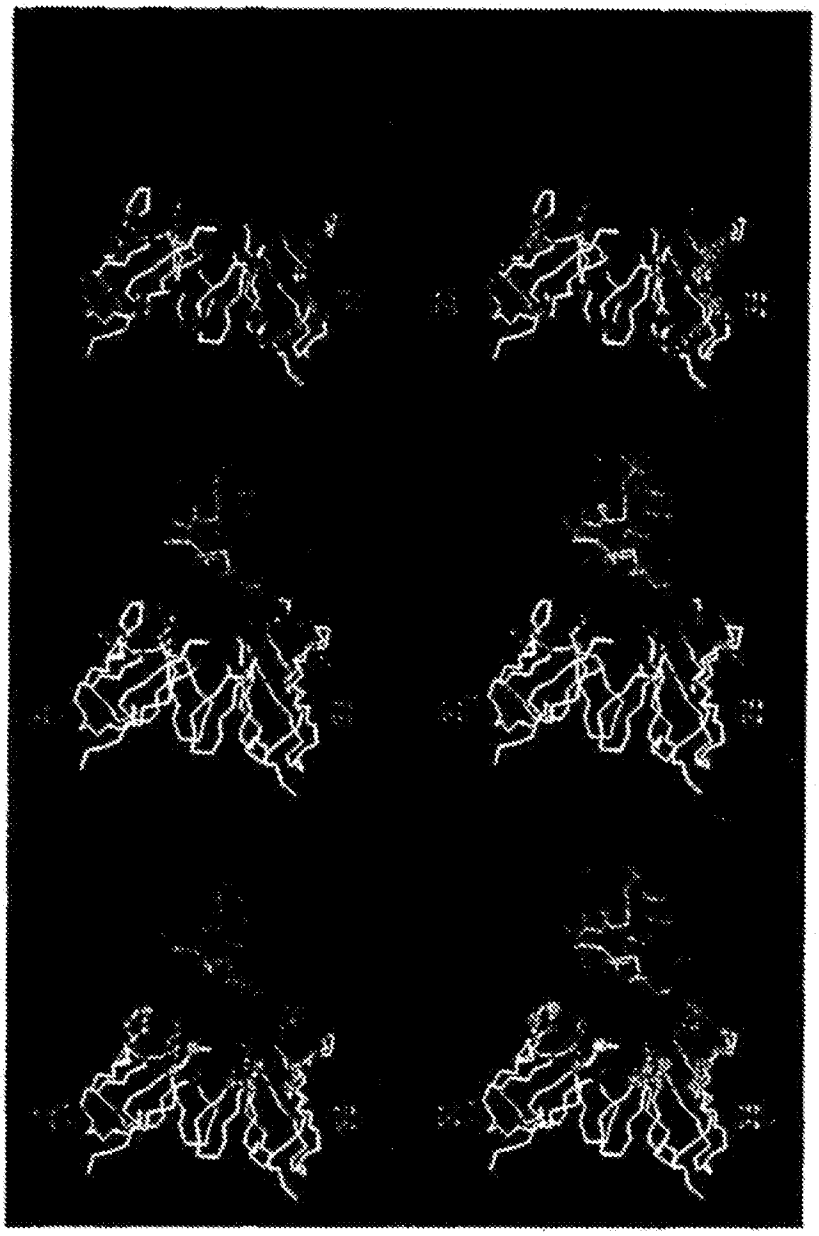

Figure 1. FabD1.3 complex with lysozyme. The α-carbon trace of the FabD1.3 (Fischmann *et al.*, 1991) is marked in white (framework region) and red (CDRs), and the α-carbon trace of lysozyme in blue. Residues corresponding to (a) differences between framework residues of mouse (D1.3) and reshaped antibody, (b) point mutations introduced into the framework of the reshaped antibody and (c) the Vernier zone, are highlighted in green.

whether there is bulky side-chain (Lys or Arg), or a smaller side-chain (Val, Ala) present (Tramontano *et al.*, 1990). We therefore changed Val71 to Lys as in D1.3.

3. Methods

(a) *Construction of reshaped light chain variable gene and Phe71 → Tyr mutant*

A myeloma expression vector used to produce engineered immunoglobulin heavy chains (Neuberger, 1983; Neuberger *et al.*, 1985) was adapted for light chain expression. This entailed synthesis and cloning the reshaped light chain V-gene and its introduction into the vector M13-HuVNP (Jones *et al.*, 1986) to replace the heavy chain variable gene.

A set of oligonucleotides was designed to encode the reshaped light chain V-gene with codon usage of mouse immunoglobulin sequences. However, the sequence encoding residues beyond number 96 of the mature protein was taken directly from the human J1 segment (Hieter *et al.*, 1982) including 30 nucleotides 5′ to the

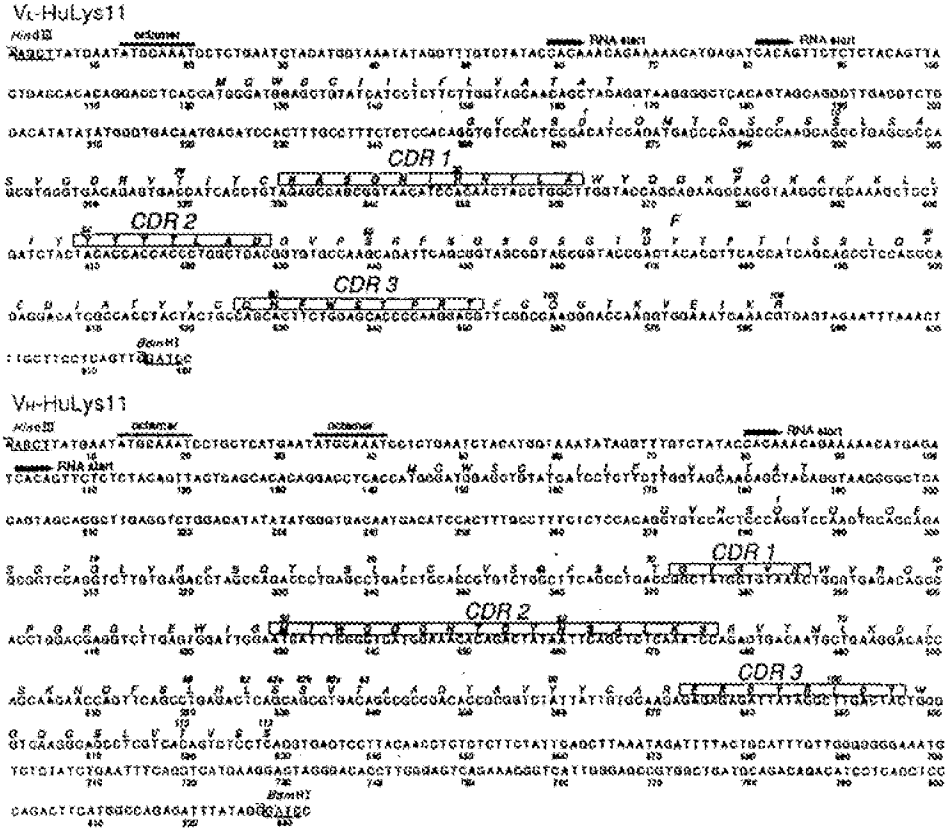

Figure 2. Nucleotide and encoded protein sequences of reshaped heavy and light chain variable domains. The DNA sequence encoding the highest-affinity reshaped antibody (HuLys11) is shown. The location of the mutations, transcriptional control motifs and protein translations appear above the corresponding nucleotide sequence, with nucleotide numbering underneath. Peptide numbering begins from the N-terminal residue of the mature protein. CDR sequences are boxed.

splice junction. Eighteen oligonucleotides were used to encode both strands of the 370 base-pair construct, and were assembled and cloned in three separate blocks, delimited by *Pst*I–*Kpn*I, *Kpn*I–*Kpn*I, and *Kpn*I–*Eco*RI sites. 50 pmol of each oligonucleotide was phosphorylated for 30 min at 37°C in a 20 μl reaction mixture with 1 mM-ATP, 5 units polynucleotide kinase, 5 mM-dithiothreitol, 50 mM-Tris, 10 mM-$MgCl_2$ (pH 8). Portions (4 μl) of each phosphorylation mixture were annealed by heating together at 80°C for 5 min, 67°C for 30 min, and cooling gradually (30 min) to room temperature. 200 nl of annealing mix was ligated into 30 ng M13-mp19 vector (Yanisch-Perron *et al.*, 1985) in a volume of 10 μl (composition as above except for 120 units of T4 DNA ligase and a pH of 7·5). Recombinant clones were sequenced and the 3 blocks excised, gel-purified and assembled by ligation into M13-mp19 as a *Pst*I–*Eco*RI fragment.

The synthetic gene was introduced as a *Pst*I–*Bam*HI fragment into the vector M13-pHVNP and joined in-frame to the signal sequence with a mutagenic oligonucleotide (5′-TCA TCT GGA TGT CGG AGT GGA CAC CT-3′) (Zoller & Smith, 1982). Further derivatives were made: about 1·2 kb of sequence 5′ to the immunoglobulin octamer transcriptional control element (Falkner & Zachau, 1984) was deleted using the oligonucleotide 5′-TAG ATT CAG AGG ATT TGC ATA TTC ATA AGC TTG GGC TAA TCA T-3′, and a point mutation, Phe71 to Tyr, was introduced using the oligonucleotide 5′-GGT GAA GGT GTA GTC GGT ACC-3′. The annotated sequence of the mutated gene is given in Fig. 2.

(b) *Construction of mutants of reshaped heavy chain variable gene*

Mutants of the reshaped heavy chain variable gene (Verhoeyen *et al.*, 1988) were constructed by oligonucleotide-directed mutagenesis. As above, 1·2 kb of sequence 5′ to the octamer motif was deleted, but here it also resulted in spurious duplication of the motif. Residues 27 to 30, initially Ser-Thr-Phe-Ser, were changed to Phe-Ser-Leu-Thr with the mutagenic oligonucleotide 5′-TAC ACC ATA GCC GGT TAA GCT GAA GCC AGA CAC GGT-3′, Ser27 to Phe with the oligonucleotide 5′-GCT GAA GGT GAA GCC AGA CAC G-3′, and Val71 to Lys with the oligonucleotide 5′-TGC TGG TGT CGT TCA GCA TTG TC-3′. The annotated sequence of the mutated gene is shown in Fig. 2.

(c) *Eukaryotic expression vectors*

Fragments carrying heavy and light chain variable genes with signal sequences and promoters (as above)

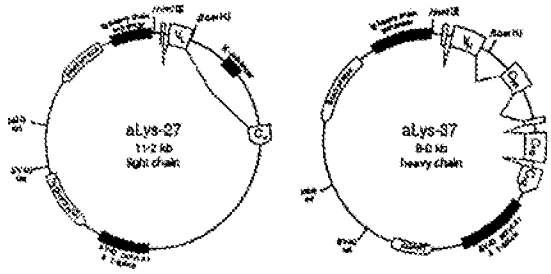

Figure 3. Vectors for expression of reshaped heavy (aLys37) and light (aLys27) chain variable regions as human γ1 and κ chains in myeloma cells. Immunoglobulin exons are indicated by wide boxes, the coding regions of β-lactamase, aminoglycoside phosphotransferase (hygromycin resistance) and bacterial xanthine-guanine phosphoribosyl transferase by narrow boxes, and splicing between immunoglobulin exons by broken lines.

were now introduced into expression vectors. A vector pSV-V_{aa}Hκ (Neuberger *et al.*, 1985) based on the vector pSV2gpt (Mulligan & Berg, 1980), was further modified to facilitate rapid cloning of the variable genes and their co-expression as heavy and light chains in cultured myeloma cells. A human κ constant gene was built into a vector utilizing hygromycin resistance as a selectable marker, and a human heavy chain γ1 gene built into a vector utilizing mycophenolic acid resistance (Fig. 3).

The assembly of the vector for light chain expression involved a ligation of 3 fragments: a 2 kb *Hin*dIII–*Bam*HI fragment containing the synthetic variable domain described above; a *Hin*dIII–*Hin*dIII fragment containing the immunoglobulin heavy chain locus 5' enhancer, β-lactamase gene, and SV40 origin of replication and promoters (M. S. Neuberger and L. Riechmann, unpublished results); a *Hin*dIII–*Bam*HI fragment containing the coding sequence of a hygromycin-specific aminoglycoside phosphotransferase, SV40 t-antigen splice site and poly(A) sequences, excised from the plasmid pSV2*hyg (A. Smith, D. Strahlow and A. Miyajima, unpublished results). Next, the vector was partially digested with *Hin*dIII, and the *Hin*dIII site at the end of the hygromycin fragment removed by fill-in extension with DNA polymerase I (Klenow fragment) and religation. The human Cκ constant region was then introduced as a *Bam*HI fragment at the unique *Bam*HI site of the vector. (A genomic fragment containing the human J and Cκ gene segments (Hieter *et al.*, 1982) was first cloned as a 10 kb *Bam*HI fragment in pUC7 (Vieira & Messing, 1982), the J-segments excised as a 5 kb *Hin*dIII fragment and the vector religated. The 5 kb *Bam*HI fragment containing the Cκ coding sequence and the κ enhancer, was used in the construction.) The *Bam*HI site at the 3' end of the Cκ constant region, and a *Hin*dIII site internal to the κ fragment were then eliminated by fill-in and religation of partial digests.

Construction of a reshaped anti-lysozyme antibody with human γ2 constant region has been described (Verhoeyen *et al.*, 1988); our interest shifted to the γ1 isotype, as it is more potent in activation of the complement cascade and of antibody-dependent cell-mediated cytotoxicity (Brüggeman *et al.*, 1987; Riechmann *et al.*, 1988). A clone of the human γ1 constant region exons (Takahashi *et al.*, 1982), was provided as a 2 kb *Bgl*II fragment in the M13 phage tg131 (Kieny *et al.*, 1983) by M. Brüggemann. After *Hin*dIII digestion, fill-in and religation to destroy the internal *Hin*dIII site, the *Bgl*II fragment was introduced into the *Bam*HI-digested pSVgpt-HuV_HLYS-HulgG2 vector (Verhoeyen *et al.*, 1988) to replace the γ2 constant region exons. Although the ligation destroys the *Bam*HI sites of the vector backbone, an internal *Bam*HI site (present in the polylinker of the M13-tg 131 vector) remains at the V-proximal end of the insert.

(d) *Construction of transfectoma lines*

Light and heavy chain constructs were introduced into myeloma cells by electroporation (Potter *et al.*, 1984), and stably transformed cells selected on the basis of drug resistance and cloned. Generally we co-transformed cells with both light and heavy chain constructs simultaneously, but we also tried transforming first with light chain, cloning the intermediate light chain producing transfectoma, then transforming with the heavy chain construct. The sequential method gave higher transfection frequencies, and was a convenient strategy in creating a family of antibodies with identical light chains, but similar yields of antibody were purified from clones obtained either through sequential or cotransformation. The level of antibody production by individual clones of cells varied widely: the better clones were identified by ELISA and picked for large scale growth.

Plasmids were purified from 1 l of bacterial culture by alkaline detergent lysis and CsCl/ethidium bromide equilibrium density gradient centrifugation (Ish-Horowicz & Burke, 1981). Heavy chain constructs were linearized with *Pvu*I, a step which increased transfection frequency by more than 10-fold. Light chain constructs do not have a convenient restriction site for linearization, so the circular form was used. The cell line NS0 (Galfré & Milstein, 1981), a myeloma which produces neither endogenous immunoglobulin chain due to abolition of heavy chain transcription and a defect in the κ transcript (Carroll *et al.*, 1988) was grown in Dulbecco's modified Eagle's medium supplemented with 10% (v/v) fetal calf serum, 110 mg sodium pyruvate/l, 100 mg streptomycin/l, and 100,000 units penicillin/l. Cells were harvested at a density of 10^6 cells/ml, and held on ice. 10^7 cells were suspended in 0·1 ml PBS or medium, placed in a sterile plastic 0·4 cm × 1 cm cuvette and mixed with 10 μg of each DNA construct. After several minutes, three 2 kV pulses from an Apelex (Bagneux, France) cell porator were applied, 1 s apart, then the cells were returned to ice. The electroporation mixture was washed into a flask with 25 ml medium, and grown overnight. An equal volume of selective medium was added, and the suspended cells distributed over a 24-well plate. For selection of hygromycin resistance alone, cells were exposed to a drug concentration of 0·4 g/l. For co-selection of hygromycin and mycophenolic acid resistance, culture medium contained 0·2 g hygromycin/l, 0·8 mg mycophenolic acid/l, and 0·25 g xanthine/l. As stock solutions of xanthine were made in 0·1 M-NaOH, an equivalent of HCl was also added to preserve the pH of the growth medium.

An antigen-based ELISA procedure was devised to facilitate screening of transformants. Microtitre plates (Dynatech) were coated overnight with 0·3 g lysozyme/l in 50 mM-$NaHCO_3$ (pH 9·6). The plates were washed with PBS, then blocked with 1% (w/v) bovine serum albumin in PBS for 5 min. 0·1 ml portions of culture supernatant were allowed to react for 2 h, and after washing, adsorbed antibody was quantified with peroxidase-conjugated rabbit anti-human IgG (Dakopatts, Denmark) diluted to

2 μg/ml in 1% bovine serum albumin/PBS. After 1 h, plates were washed and substrates for the colour reaction added: 4 mM-H_2O_2, 1 mM-diammonium 2, 2'-azino bis (3-ethylbenzthiazoline sulphonic acid), in 0·1 M-citrate buffer (pH 4·5). For screening of light chain producing transfectomas, a similar procedure was used. Plates were coated with a 1:500 dilution of ascites fluid of the anti-human kappa hybridoma NH3/41 (Downie *et al.*, 1983), supplied by J. Jarvis. Peroxidase-conjugated rabbit anti-human kappa was used for quantitation.

Once visible colonies had appeared in the 24-well plates, after 2 weeks incubation, antibody production was assayed by ELISA. Cells from wells giving the strongest signals were cloned by limiting dilution in selective medium and regrowth on 96-well plates. The ELISA screening was repeated, usually on 20 or more clones, and the cell lines giving the strongest signals retained for permanent storage and large-scale growth for antibody production.

(e) *Antibody production*

Antibodies were purified to homogeneity from several litres of culture medium by affinity chromatography on both lysozyme-Sepharose and Protein A-Sepharose.

Sepharose CL-4B (Pharmacia), chilled in 1 M-Na_2CO_3, was activated for 2 min with 200 mg CNBr per ml resin, added as 1:1 solution in CH_3CN. The buffer was changed to 0·1 M-$NaHCO_3$, 0·5 M-NaCl (pH 8·5), and 5 mg lysozyme per ml. Sepharose was added, as a 1% solution in 10 mM-acetate, 40 mM-NaCl (pH 4·0). The slurry was stirred intermittently for 4 h and then residual imidocarbonate groups hydrolysed by overnight treatment with 0·1 M-$NaHCO_3$ (pH 10·0). To minimize the effect of leakage of the immobilized lysozyme during chromatography, the columns were washed with high-salt and elution buffers immediately before use. The lysozyme-Sepharose columns were used once and discarded. Protein A-Sepharose was washed with 0·1 M-citric acid before use; resin was in this case re-used.

Transfectoma cultures were grown from cloned stocks in flasks to 100 to 200 ml, in medium with both mycophenolic acid and hygromycin present, and 10% fetal calf serum. Each culture was then transferred to a roller bottle, and grown to 2 l with 5% serum with mycophenolic acid. Cells were grown until the culture medium was exhausted, leading to the demise of most cells. Cultures were cleared by centrifugation at 11,000 *g* for 15 min. Solid $(NH_4)_2SO_4$ was added slowly at a ratio of 0·313 kg/l of supernatant, and the mixture stirred for 1 h at 4°C. Precipitate was harvested by a 45 min centrifugation dissolved in 20 ml phosphate buffered saline (125 mM-NaCl, 6·4 mM-NaH_2PO_4, 16·6 mM-Na_2HPO_4) (PBS) and dialysed against the same.

The dialysed protein was centrifuged to remove any insoluble material, and the reshaped antibodies applied to a 5 ml column of lysozyme-Sepharose, previously equilibrated in PBS. The column was washed extensively with high-salt buffer, 0·1 M-Tris, 0·5 M-NaCl (pH 8·5), and antibody eluted with 50 mM-diethylamine. 1 M-Tris·HCl (pH 7·4) was present in fraction collector tubes to neutralize the eluate. The eluate was then applied directly to a 5 to 10 ml Protein A-Sepharose column equilibrated in PBS. The columns were washed, eluted with 4 column vols of a gradient, 0·1 M-Na_3-citrate to 0·1 M-citric acid, and the antibody dialysed against PBS, 0·2 mM-EDTA.

For purification of the D1.3 antibody (mouse γ1 isotype) on Protein A-Sepharose, the sample was dialysed against either 3 M-NaCl, 0·1 M-glycine (pH 8·9), or against 0·1 M-Na_2HPO_4 (pH 8), before application to the column equilibrated in fresh dialysis buffer, and eluted with 0·1 M-citrate (pH 6).

Prior to storage, antibody was checked on an SDS/polyacrylamide gel (Laemmli, 1971) to verify purity, and an ultraviolet spectrum taken to ascertain concentration. Yields of purified antibody were approximately 15 mg/l of culture in the case of the hybridoma, and typically 2 to 3 mg/l for the transfectoma lines. Antibody solutions were filter-sterilized and stored at 4°C under N_2 in acid-washed septum-top vials.

(f) *Physical methods*

The conditions chosen for all physical measurements were a temperature of 20°C and a standard buffer of 25 mM-NaH_2PO_4, 125 mM-NaCl, 0·2 mM-EDTA (pH 7·0). Ultraviolet extinction coefficients ($\varepsilon_{280\,nm}$) were determined for the mouse and reshaped antibodies to facilitate routine, accurate determination of concentration. Quantitative amino acid analysis was performed on samples of known optical density, with norleucine added prior to hydrolysis as an internal standard. Correlation of the observed amino acid composition with that deduced from the encoded protein sequence gave $\varepsilon_{280\,nm}$ values of $2{\cdot}2 \times 10^5$ (M^{-1} cm^{-1}) for mouse and $2{\cdot}1 \times 10^5$ (γ2 isotype) or $1{\cdot}9 \times 10^5$ (γ1 isotype) for reshaped antibodies. Antibody preparations were quantified at the time of storage. Portions were withdrawn as needed and used directly, assuming that the concentration at the time of storage was unchanged. Hen egg lysozyme and bovine ubiquitin were from Sigma. These were dissolved in PBS and dialysed against the same buffer. Concentrations were determined spectrophotometrically, using $\varepsilon_{280\,nm}$ of 37,600 for lysozyme (Imoto *et al.*, 1972*a*) and 0·16 $(mg/ml)^{-1}$ cm^{-1} for ubiquitin (Cinchanover *et al.*, 1980).

(g) *Fluorescence spectroscopy*

Emission spectra revealed a large quench of native Trp fluorescence upon antibody-lysozyme complex formation; fluorescence measurements at fixed wavelengths were then used to determine the stoichiometry and approximate equilibrium constant.

A Perkin-Elmer LS-5B spectrofluorimeter interfaced to a Macintosh computer was used for all measurements. Of significance was the 50 Hz stroboscopic Xe light source, which gives a 150 W pulse, but has a root-mean-square intensity of 8 W, reducing photobleaching of samples to negligible levels. There was virtually no signal drift over the course of an experiment. Temperature control of the cuvette block was maintained by a thermostatted circulating water bath.

For emission spectra, an excitation wavelength of 280 nm was used, with a bandwidth of 10 nm; the emission bandwidth was 5 nm. Samples were scanned from 300 to 420 nm at 50 nm/min, with an 8 s time constant. In a typical set of measurements, a buffer sample was scanned to obtain a baseline. Antibody was added to 100 nM for the next scan, following which lysozyme was added in a negligible volume to 200 nM. A 3rd scan was taken after a 2 min wait for complex formation to occur. Similar measurements were made on a separate sample of buffer, then 200 nM-lysozyme alone. The spectra of protein samples were then corrected by numerical subtraction of the buffer blank.

In a typical titration, 15 samples of a concentrated lysozyme solution were added to a 3 ml sample of 10 to 200 nM-antibody, culminating in a molar ratio of 4 lysozyme/antibody (i.e. 2 lysozyme added per combining site).

For higher antibody concentrations, a minimum interval of 2 min was maintained between adding lysozyme and reading the fluorescence. For lower concentrations, consideration was made of the length of time necessary for approach to equilibrium. An approximate relaxation time was estimated from any available kinetic and equilibrium data, and an interval several times that used, often in excess of 5 min. Titrations were most frequently done at an excitation wavelength of 280 nm and an emission wavelength of 400 nm. The excitation bandwidth was 10 nm. Emission bandwidths of 5, 10 or 20 nm were used, the choice for a given experiment depending on the magnitude of sample fluorescence. Each observation was obtained by averaging the fluorescence signal over a span of 16 s.

A source of systematic error in titrations was a progressive loss of fluorescence perhaps by adsorption to glass. This was especially compromising at high dilutions of antibody. For example, the fluorescence of a 10 nM solution of D1.3 antibody decreased 25% during a mock titration with samples of buffer. Use of ubiquitin as a carrier almost completely overcame this artifact. Ubiquitin has no tryptophan residues and a single tyrosine (Schlesinger *et al.*, 1975), hence is very weakly fluorescent. A concentration of 30 μg/ml gave a stable background, which was a fraction of the total fluorescence of the antibody and antigen. Discounting background, the fluorescence, F, of a mixture of antibody and lysozyme at equilibrium is described by the equation:

$$F = f_{Ab} rA + f_{Lys} L - f_\Delta \tfrac{1}{2}\{rA + L + K) - \sqrt{(rA + L + K)^2 - 4rAL}\}, \quad (1)$$

where A and L are the total (complexed and uncomplexed) antibody and lysozyme concentrations; r is the average number of combining sites per antibody molecule; f_{Ab} and f_{Lys} are the molar fluorescence of free antibody (on a per-site basis) and lysozyme; f_Δ is the molar fluorescence change occurring on complexation of lysozyme, a positive value indicating a net quench; K is the equilibrium constant for complex dissociation. A computer program for analysis of experimental data according to eqn (1) was written in Pascal and implemented on the Apple Macintosh computer. A and L were treated as independent variables, F as the dependant variable, and f_{Ab}, f_{Lys}, f_Δ, r and K were adjustable parameters optimized by the operation of the Marquardt least-squares algorithm on a first-order Taylor series expansion of eqn (1).

(b) *Rapid kinetics*

Measurement of the rate of antibody–antigen association was determined from a series of stopped-flow measurements under a pseudo-first-order regime. A commercial instrument of standard design (Hi-Tech Scientific, Salisbury, U.K.) was used for this work, in fluorescence mode. Light from a 75 W Xe lamp passed through a monochromator set at 280 nm, and thence *via* a light guide to the sample. Light emitted from the sample passed through a 320 or 360 nm cutoff (lower limit) filter before impinging on the photomultiplier. A Hewlett-Packard 310 computer fitted with an analogue-digital converter served for data capture and analysis, using a software package supplied by the stopped-flow manufacturer. Syringes and reactant reservoirs were bathed in water from a thermostatted circulating bath. The applied voltage on the photomultiplier was generally near 1·2 kV, giving a signal voltage of 1 to 6 V.

For measurement of on-rates, two 1 ml syringes were used, one with 100 nM-antibody, the other with 2, 4, 6 or 8 μM-lysozyme. A 20 nm excitation slit was used for high intensity. For a single observation, 50 μl portions of each reactant were mixed under maximum pneumatic pressure, and fluorescence data collected for a period chosen (after preliminary runs) to be approximately 6 half-lives. Ten or more transients were averaged prior to least-squares fitting to a simple exponential.

(i) *Equilibrium constant determination*

The method is based on a concept described by Segal (1975). A pseudo-equilibrium is established by a dilution in a stopped-flow instrument. The functional site concentration of an antibody preparation is first calibrated by titration with antigen. A mixture containing antibody at 11 times a notional pseudo-equilibrium concentration, on a site basis, and antigen at 22 times this concentration is allowed to equilibrate, then placed within a 0·25 ml stopped-flow syringe. A 2·5 ml syringe is filled with antibody alone, at 1·1 times the notional concentration. As the drive syringes are of proportional cross-sectional area, equal translation of their plungers configures an 11-fold dilution of the concentrated antibody and lysozyme mixture, and a 1·1-fold dilution of the free antibody solution, thus establishing a pseudo-equilibrium mixture with all 3 components, antibody, lysozyme and complex, approximating the notional concentration. For a single observation, a combined reactant volume of 100 μl was mixed, and data collected for 20 or 50 s.

A 10 nm excitation slit was employed to reduce photobleaching, and the longest available time constant, 100 ms, was used for signal stabilization. Traces for multiple identical runs were averaged, and fitted to an exponential. The amplitude of the exponential was taken as the fluorescence change, ΔF_∞, on relaxation of the initial mixture to a true equilibrium. The equilibrium constant, K, was determined by least-squares analysis as described in Results section (c).

4. Results

(a) *Fluorescence spectroscopy*

Fluorescence emission spectra were taken of lysozyme, the set of anti-lysozyme antibodies, and antibody–antigen mixtures (see legend to Fig. 4). As is evident from the spectra in Figure 4(a), the fluorescence intensity observed from the mixtures was considerably less than the sum of intensities of the two separate components. Indeed, over much of the spectral range examined, the magnitude of this quench exceeded the fluorescence emission of free lysozyme, resulting in a decrease of fluorescence upon addition of antigen. The quench was not due to an "inner filter" effect as it was seen at low absorbance ($A_{280\,nm} = 0{\cdot}02$).

This quench at different wavelengths of emission is presented in Figure 4(b) in the form of a fluorescence difference spectrum, and also as a fraction of the total fluorescence. The peak of the difference spectrum, at 349 nm, is red-shifted from the maxima (<340 nm) of either antibody or antigen spectrum indicating that the quenched residues are in a polar environment (Van Duuren, 1961). Lysozyme has six Trp residues; however, more than 80% of the Trp fluorescence may be attributed to

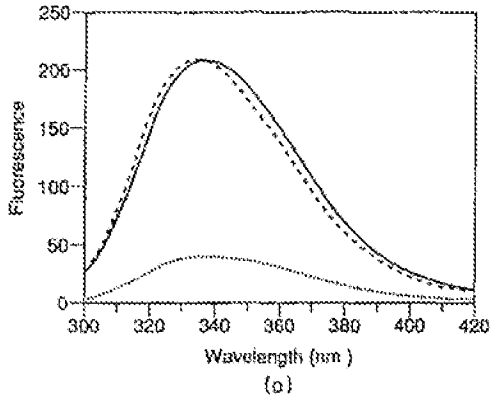

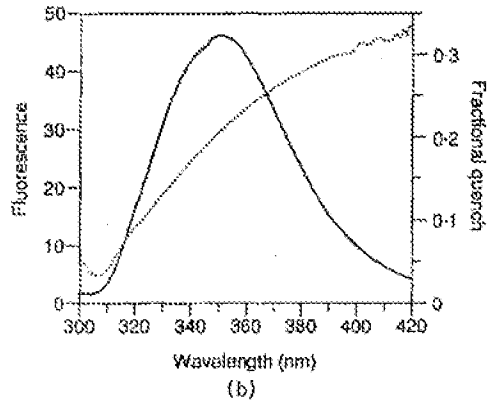

Figure 4. Fluorescence spectroscopy of D1.3 antibody and complex with lysozyme. (a) Fluorescence emission spectra of 100 nM D1.3 (continuous line), 200 nM-lysozyme (dotted line), and mixture at the same concentrations (broken line). (b) Difference and ratio spectra. A fluorescence difference spectrum (continuous line, left ordinate scale) was calculated by subtraction of the observed signal of lysozyme D1.3 mixture from the sum of the fluorescence of free D1.3 and lysozyme. The fractional quench (dotted line, right scale) was calculated as the ratio of this difference to the sum.

residues 62 and 108 (Imoto *et al.*, 1972*b*), neither of which is near the antibody–antigen interface. There are two light chain and four heavy chain Trp residues in cognate positions of the variable domains of D1.3 and the humanized antibodies. Of these, Trp62 of the light chain and Trp52 of the heavy chain make direct contacts to Arg125 and Asp119 of lysozyme, and are the likely origin of the quench effect. For the reshaped antibodies, the peak of the difference spectrum was also red-shifted, ranging from 350 to 363 nm.

The quench as a fraction of total fluorescence (Fig. 4(b)) increases monotonically with wavelength, reaching 30% at 400 nm in the case of D1.3. The reshaped antibodies yielded qualitatively similar spectra but the magnitude of the quench was generally lower (20%).

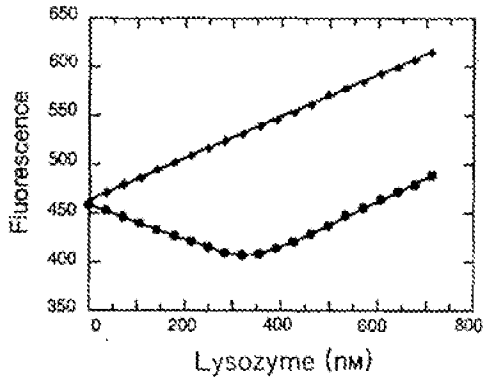

Figure 5. Titration of D1.3 antibody with lysozyme. Small samples of a concentrated lysozyme solution were added to 200 nM-D1.3 (–●–●–) and fluorescence emission measured at 390 nm. A control antibody (320 nM) with no specificity for lysozyme was titrated in parallel (–◆–◆–).

(b) *Fluorescence titrations and stoichiometries*

Antibody samples were titrated with lysozyme and fluorescence monitored at fixed wavelengths. Because a high fractional quench was more significant than the overall fluorescence signal in determining the sensitivity of these measurements, emission wavelengths of 390 to 400 nm were used, rather than the lower values corresponding to the maxima of the emission or difference emission spectra. Figure 5 shows the titration of D1.3 in parallel with a control antibody that does not bind lysozyme. Additions to the control gave a linear increase in fluorescence over the entire range of lysozyme concentrations. By contrast, as D1.3 was titrated, the fluorescence decreased until a stoichiometry of about two antigen molecules per antibody was reached, beyond which the signal rose linearly with the same slope as the control. Titrations of the reshaped antibodies gave similar data with varying curvature at the breakpoint. The observed stoichiometry of the antibodies with lysozyme, and absence of quench with the control, indicated that the spectral change arose from the combination of one molecule of lysozyme with each antigen binding site.

The curvature at the breakpoint depends on the affinity of the particular antibody for lysozyme. Fluorescence titration data were fitted to equation (1) to derive stoichiometries and equilibrium constants. The D1.3 sample in Figure 5 showed 1·82 antigen binding sites per antibody molecule, and other antibodies generally fell in the range 1·6 to 2·1 sites per molecule. The method gave highly reproducible stoichiometries. The equilibrium constants, however, were erratic, and often had large standard deviations. The pseudo-equilibrium relaxation method detailed in the next section thus was developed as a means of getting more reliable affinity data.

(c) *Equilibrium constants*

Suppose that a 1 : 1 : 1 mixture of free antibody, free lysozyme, and antibody–lysozyme complex could be created artificially, and the concentrations of the components followed as the system relaxes to a true equilibrium. In the ideal mixture, if the pseudo-equilibrium concentration of the three reactants is greater than the dissociation constant, a net association of antibody and antigen would occur; if lower, there would be a net dissociation of the complex. When the pseudo-equilibrium concentration exactly matches the true equilibrium constant there would be no net change. By measuring changes in fluorescence on mixing, we could then estimate the equilibrium constant from the cross-over point, at which there is no change in fluorescence.

In practice we try to make the three equimolar reactants by mixing a concentrated lysozyme (2 molar equivalents): antibody (1 molar equivalent of binding site) solution with a dilute solution of free antibody (1 molar equivalent). Because the binding of antibody and antigen is not infinitely tight, we do not fulfil the ideal starting conditions: the actual concentration of complex, C, is given by the equation (2):

$$C = \tfrac{1}{2}\{(rA + L + K) - \sqrt{(rA + L + K)^2 - 4rAL}\} \quad (2)$$

where the symbols are as for equation (1). The change in fluorescence ΔF_∞ occurring after mixing the two solutions is:

$$\Delta F = -f_\Delta \left\{\frac{C_0}{\mathrm{dil}} - C_\infty\right\} \quad (3)$$

where C_0 and C_∞ are given by equation (2), respectively, for the 2 : 1 cocktail prior to mixing and the full reaction mixture after complete re-equilibration, and d is the factor by which the concentrated solution is diluted. The fluorescence change is thus a function of K_d and we can calculate K from a least-squares fit of experimentally determined ΔF values to equation (3).

Dissociation constants were determined for each of the reshaped antibodies by pseudo-equilibrium relaxation, and the values obtained are listed in Table 1. The results for HuLys0 are shown in Figure 6. In this case it was possible to approach the equilibrium from both directions (both positive and negative fluorescence changes), and the least-squares analysis indicates a dissociation constant of 260 nM. The precision of this technique in determining equilibrium constants proved superior to using fluorescence titration or the ratio of forward and reverse kinetic rate constants.

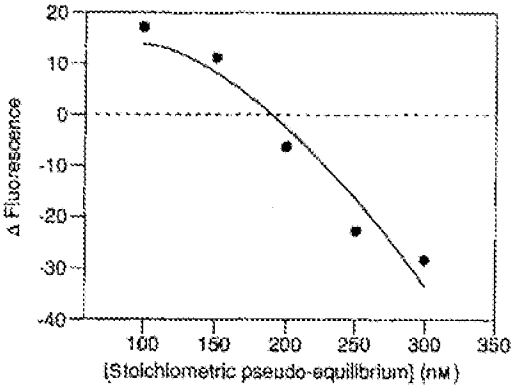

Figure 6. Determination of affinity constant of HuLys0 reshaped antibody for lysozyme by pseudo-equilibrium relaxation. Antibody and antibody with lysozyme solutions were mixed as described in the text, to give the "pseudo-equilibrium" concentration. This is a notional value, equal to the concentration of free antibody sites, free antigen and complexed antigen which would occur upon mixing in the limit of infinitely tight antibody–antigen interaction. The fluorescence change occurring after mixing is plotted in the ordinate. The curve is calculated from parameters derived by least-squares analysis of the experimental points.

HuLys0, the prototype reshaped antibody, has an affinity in the range expected for an antibody in a primary immune response, but nearly two orders of magnitude weaker than D1.3. Framework substitutions effected significant increases in antigen affinity. The data in Table 1 are presented in a

Table 1

Physical constants of anti-lysozymes

Antibody	k_{on} (mol^{-1} l s^{-1}/10^6)	K_d (nM)	Residue substitutions				Isotype
			V_K : 71	V_H : 27	29	71	
D1.3	1·36 (0·02)	3·7 (1·8)	Y	F	L	K	—
HuLys0	0·68 (0·02)	260 (16)	F	S	F	V	γ2
HuLys3	1·18 (0·03)	64 (13)	Y	S	F	V	γ2
HuLys6	1·45 (0·12)	48 (9)	Y	F	F	V	γ1
HuLys7	1·33 (0·10)	77 (4)	Y	S	F	V	γ1
HuLys8	1·26 (0·10)	26 (5)	Y	F	L	V	γ1
HuLys9	0·63 (0·03)	120 (7)	F	F	L	V	γ1
HuLys10	1·33 (0·12)	18 (8)	Y	F	F	K	γ1
HuLys11	1·31 (0·12)	14 (2)	Y	F	L	K	γ1

Parenthetical values are standard errors.

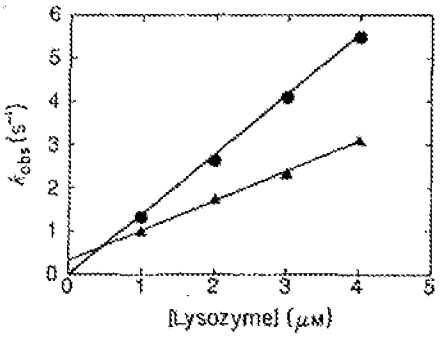

Figure 7. Kinetics of antigen binding. 50 nM-D1.3 (--●--●--) or HuLys0 (--▲--▲--) was reacted with excess lysozyme in a stopped-flow instrument. The observed pseudo-first order rate constant is plotted against the corresponding lysozyme concentration. The slope of the regression lines corresponds to the second order rate constant for antibody–antigen association.

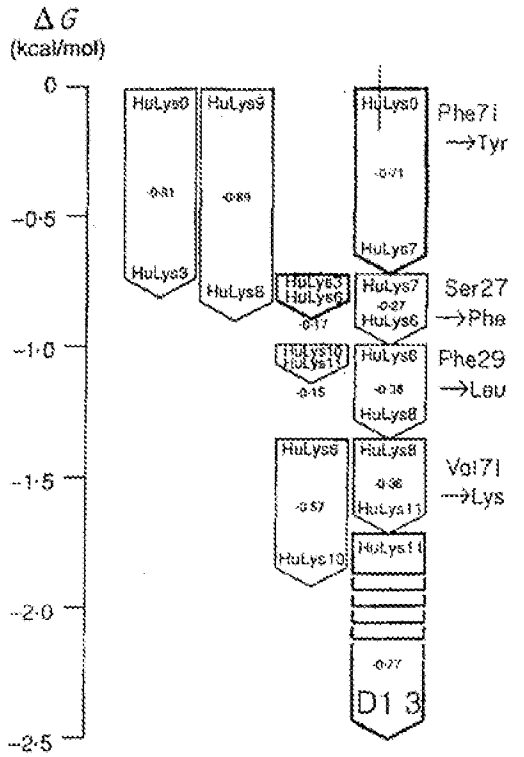

Figure 8. Energetic effect of framework substitutions. Differences in free energy of association were calculated for pairs of antibodies (using $\Delta G = -RT \ln K_1/K_2$) from the equilibrium constants in Table 1. Each of the boxes denotes the difference in free energy of lysozyme binding resulting from mutation. The boxes can be built into a train reflecting the energetic changes of a sequential transformation of the weakest affinity antibody, HuLys0, into the strongest, D1.3. A shaded outline denotes molecules differing in constant region isotype. Several of the comparisons are not strictly single-site mutations. The heavy chain mutation Phe29 to Leu was co-ordinated with 2 others, such that reshaped antibodies had either the sequence Thr28-Phe29-Ser30 or Ser28-Leu29-Thr30. The side-chains of residues 28 and 30 lie on the surface and they do not appear to interact with the remainder of the antibody (Fischmann *et al.*, 1991).

different form in Figure 8. A free energy scale denotes changes in free energy of association with antigen, starting from HuLys0. The progression HuLys0-7-6-8-11 represents a systematic addition of single-step changes in the variable domains, ignoring changes in isotype from human γ1 to γ2 antibodies (HuLys0 to HuLys7) and changes at V_H 28 and 30 (HuLys6 to HuLys8) which are probably irrelevant to binding affinity (see Discussion). A final step in Figure 8, from HuLys11 to D1.3, denotes the energetic gain that would accrue from a further 42 mutations to restore the mouse framework regions. The four mutations introduced into the human framework regions thus recoup two-thirds of the antigen-binding free energy lost in the initial CDR transplant.

(d) *Kinetics of antigen binding*

It was possible to follow the kinetics of binding from the fluorescence changes on complex formation. Antibody was mixed with a 10 to 40-fold excess of lysozyme per site, and the reaction followed for periods of up to two seconds. The resulting fluorescence change in all cases followed a simple exponential allowing a pseudo-first order rate constant to be abstracted by least-squares analysis. The observed rate constants were in turn plotted against the concentration of lysozyme used (Fig. 7), and the slope of the resulting line taken as the second order rate constant for bimolecular association (on-rate). On-rates are listed along with equilibrium dissociation constants in Table 1. The D1.3 antibody binds lysozyme with a rate constant of $1{\cdot}4 \times 10^6$ l mol^{-1} s^{-1}, as do several of the reshaped antibodies. This indicates that the initial recognition event is identical, despite differences in affinity that are largely controlled by the off-rate. However, two of the reshaped antibodies have slower on-rates, correlating with light chains with Phe71.

In Figure 7 the ordinate intercept of the line corresponds to the off-rate. For D1.3, the line appears to intersect the origin (due to slow off-rate) and the off-rate cannot be determined in this way. However, for HuLys0, the off-rate is faster, and the intercept is displaced further from the origin and can be determined. The off-rate values that could be determined in this way (HuLys0 and HuLys9) were consistent with those calculated from k_{on} and K (determined independently as above). The D1.3–lysozyme complex dissociates with a calculated half-life of 134 seconds, contrasting with a four second bound lifetime for HuLys0, the weakest binder.

5. Discussion

Here we have described the expression of anti-lysozyme reshaped antibodies (Jones *et al.*, 1986; Verhoeyen *et al.*, 1988; Riechmann *et al.*, 1988) as human γ1, κ isotypes in myeloma cells. Variable region expression cassettes, including Ig promoter, signal and splice sites, were built in M13 vectors to facilitate oligonucleotide-directed mutagenesis. These cassettes were readily cloned into pSV vectors (Mulligan & Berg, 1980; Neuberger, 1983) carrying human γ1 and κ genes for expression of antibody. These M13 and pSV vectors have general utility, and aspects of this work have already been reported by Riechmann *et al.* (1988) and Orlandi *et al.* (1989) as unpublished results.

We also describe several methods, using fluorescence quench on antigen binding, for the determination of antibody affinity, kinetics and stoichiometry of binding. Hitherto the use of fluorescence quench to study the interaction of protein antigens with antibody has involved the chemical coupling of spectral probes to antibody or antigen. Here we use the changes in fluorescence of tryptophan residues on forming the antigen–antibody complex to follow the interaction. This allowed the accurate determination of equilibrium constants of the antibody–lysozyme interaction, and this proved essential for following the small energetic changes between mutants.

Antibody variable domains comprise a framework of β-sheet surmounted with antigen-binding loops that can be transplanted between antibodies. However, some amino acids of the framework appear to make important interactions with the loops (Chothia & Lesk, 1987). We attempted to dissect their contribution by "rebuilding" the antigen-binding affinity of a reshaped anti-lysozyme antibody (K = 200 nM), and have focussed on four framework substitutions, V_κ Phe71 → Tyr, V_H Ser27 → Phe, Phe29 → Leu and Val71 → Lys. The reasons for designing these substitutions are given in Materials and Methods. We found that the lost affinity could be rebuilt to 14 nM by introducing all these mutations, to within a factor of four of the original mouse antibody (3·7 nM). However, each mutation alone made a small contribution to the enhanced affinity. V_κ Phe71 → Tyr had the greatest effect and was unique in increasing the rate constant for association; the other changes only affected the rate of dissociation of the antibody–antigen complex.

The residues 27, 29 and 71 in the heavy chain form a contiguous triad, in which Phe27 and Leu29 side-chains and the hydrophobic portion of the Lys71 side-chain interact together, and with the loops CDR 1 and 2 (Amit *et al.*, 1986). The energy diagram (Fig. 8) suggests that these residues do not behave independently on supporting the loops in antigen binding. For example, comparing the two sites at residues 29 and 71 of the heavy chain, the energetics of the changes (Phe29 → Leu) or (Val71 → Lys) depend on the precise residue at the other site. However, comparing the two sites at residue 27 of the heavy chain and 71 of the light chain, the energetics of the change (Phe71 → Tyr) are independent of the precise residue at the other site.

Table 2
Residues in the "Vernier" zone (Kabat numbering)

Heavy chain	Light chain
2	2
27–30	4
47–49	35–38
67	46–49
69	64
71	66
73	68–69
78	71
93–94	98
103	

These residues are examples of a more general subset of framework residues acting as a "Vernier" zone (Fig. 1(c)), which may adjust CDR structure and fine-tune the fit to antigen. In Table 2 we list framework residues forming a layer underlying the CDRs and that are positioned to exert these effects. From inspection of known crystal structures, such roles have been ascribed to heavy chain residue 71 (Tramontano *et al.*, 1990), and implicitly to residues 27 to 30, which form part of an antigen-binding loop (Chothia & Lesk, 1987). Such roles are also consistent with the altered binding properties of antibody mutants. Independent studies of anti-digoxin (Panka *et al.*, 1988; Novotny *et al.*, 1990) and anti-phosphorylcholine (Chien *et al.*, 1989) antibodies drew attention to the specific interaction of heavy chain framework residue 94 with heavy chain CDR residue 101.

The Vernier zone has an obvious consequence for the design of humanized antibodies. Although grafting CDRs onto a single set of acceptor frameworks may well transfer the antigenic specificity of the donor antibody (Jones *et al.*, 1986), ideally the Vernier residues should also be matched. Indeed substitutions of these residues have been shown to be important to restoring the affinity in CDR grafted antibodies, for example in heavy chains residue 27 in the antibodies CAMPATH-1 (Riechmann *et al.*, 1988) and D1.3, residue 71 in D1.3, residue 94 in anti-RSV (Tempest *et al.*, 1991); in light chains residue 71 in D1.3.

In view of the structural role for residues of the Vernier zone in supporting CDR loop conformations and/or their relative dispositions, alterations at these points may have some role in affinity maturation. Arg94 of the V-186.2 heavy chain of the anti-nitrophenacetyl response is frequently changed to Thr (Blier & Bothwell, 1987; Allen *et al.*, 1988). Likewise residue 36 of the V_κ-Ox1 anti-phenyloxazolone light chain consistently mutates from Tyr to Phe (Griffiths *et al.*, 1984). This residue appears to support the local CDR structure and to interact

directly with hapten (Alzari *et al.*, 1990). In the T15 anti-phenyl-oxazolone heavy chain, residue 49 commonly changes from Gly to Ala or Val (Berek *et al.*, 1985). Furthermore, we note that closely related germline genes (see Pascual & Capra, 1991, for a compilation of sequences) can differ at one or several of these sites, suggesting that variability of these residues may also be a component of the diversity of structures found in the primary antibody repertoire.

We thank Roberto Poljak for D1.3 co-ordinates, Martine Verhoeyen for the D1.3 nucleotide sequence, and Marianne Brüggeman, Philip Leder, Michael Neuberger and Andrew Smith for vector parts. We also acknowledge Cyrus Chothia, Tom Creighton and César Milstein for valuable discussions. J.F. was a Fellow of the Jane Coffin Childs Fund for Medical Research, and a Merck Fellow.

References

Allen, P. M., Matsueda, G. R., Haber, E. & Unanue, E. R. (1985). Specificity of the T cell receptor: two different determinants are generated by the same peptide and the I-A^k molecule. *J. Immunol.* 135, 368–373.

Allen, D., Simon, T., Sablitzky, F., Rajewsky, K. & Cumano, A. (1988). Antibody engineering for the analysis of affinity maturation of an anti-hapten response. *EMBO J.* 7, 1995–2001.

Alzari, P. M., Spinelli, S., Mariuzza, R. A., Boulot, G., Poljak, R. J., Jarvis, J. M. & Milstein, C. (1990). Three-dimensional structure determination of an anti-2-phenyloxazolone antibody: the role of somatic mutation and heavy/light chain pairing in the maturation of an immune response. *EMBO J.* 9, 3807–3814.

Amit, A. G., Mariuzza, R. A., Phillips, S. E. V. & Poljak, R. J. (1986). Three-dimensional structure of an antigen-antibody complex at 2·8 Å resolution. *Science*, 233, 747–753.

Berek, C., Griffiths, G. & Milstein, C. (1985). Molecular events during maturation of the immune response to oxazolone. *Nature (London)*, 316, 412–418.

Bhat, T. N., Bentley, G. A., Fischmann, T. O., Boulot, G. & Poljak, R. J. (1990). Small rearrangements in structures of Fv and Fab fragments of antibody D1.3 on antigen binding. *Nature (London)*, 347, 483–485.

Blier, P. & Bothwell, A. (1987). A limited number of B cell lineages generates the heterogeneity of a secondary immune response. *J. Immunol.* 139, 3996–4006.

Brüggeman, M., Williams, G. T., Bindon, C. I., Clark, M. R., Walker, M. R., Jefferis, R., Waldmann, H. & Neuberger, M. S. (1987). Comparison of the effector functions of human immunoglobulins using a matched set of chimeric antibodies. *J. Exp. Med.* 166, 1351–1361.

Carroll, W. L., Mendel, E. & Levy, S. (1988). Hybridoma fusion cell lines contain an aberrant kappa transcript. *Mol. Immunol.* 25, 991–995.

Chien, N. C., Roberts, V. A., Giusti, A. M., Scharf, M. D. & Getzoff, E. D. (1989). Significant structural and functional change of an antigen-binding site by a distant amino acid substitution: proposal of a structural mechanism. *Proc. Nat. Acad. Sci., U.S.A.* 86, 5532–5536.

Chothia, C. & Lesk, A. M. (1987). Canonical structures for the hypervariable regions of immunoglobulins. *J. Mol. Biol.* 196, 901–917.

Ciechanover, A., Elias, S., Heller, H., Ferber, S. & Hershko, A. (1980). Characterization of the heat-stable polypeptide of the ATP-dependent proteolytic system from reticulocytes. *J. Biol. Chem.* 255, 7525–7528.

Co, M. S., Deschamps, M., Whitley, R. J. & Queen, C. (1991). Humanized antibodies for antiviral therapy. *Proc. Nat. Acad. Sci., U.S.A.* 88, 2869–2873.

Downie, D. M., Voak, D., Jarvis, J., Waldman, H. & Spitz, M. (1983). The use of monoclonal antibodies to human IgG in blood transfusion serology. *Biotest Bull.* 4, 348–352.

Epp, O., Colman, P., Fehlhammer, H., Bode, W., Schiffer, M., Huber, R. & Palm, W. (1974). Crystal and molecular structure of a dimer composed of the variable portions of the Bence-Jones protein REI. *Eur. J. Biochem.* 45, 513–524.

Falkner, F. G. & Zachau, H. G. (1984). Correct transcription of an immunoglobulin κ gene requires an upstream fragment containing conserved sequence elements. *Nature (London)*, 310, 71–74.

Fischmann, T. O., Bentley, G. A., Bhat, T. N., Boulot, G., Mariuzza, R. A., Phillips, S. E. V., Tello, D. & Poljak, R. J. (1991). Crystallographic refinement of the three-dimensional structure of the FabD1.3-lysozyme complex at 2·5 Å resolution. *J. Biol. Chem.* 266, 12915–12920.

Galfré, G. & Milstein, C. (1981). Preparation of monoclonal antibodies: strategies and procedures. *Methods Enzymol.* 73, 3–46.

Gorman, S. D., Clark, M. R., Routledge, E. G., Cobbold, S. P. & Waldmann, H. (1991). Reshaping a therapeutic CD4 antibody. *Proc. Nat. Acad. Sci., U.S.A.* 88, 4181–4185.

Griffiths, G. M., Berek, C., Kaartinen, M. & Milstein, C. (1984). Somatic mutation and the maturation of immune response to 2-phenyl oxazolone. *Nature (London)*, 312, 271–275.

Hale, G., Dyer, M. J. S., Clark, M. R., Phillips, J. M., Marcus, R., Riechmann, L., Winter, G & Waldmann, H. (1988). Remission induction in non-Hodgkin lymphoma with reshaped human monoclonal antibody CAMPATH-1H. *Lancet*, 2, 1394–1399.

Harper, M., Lema, F., Boulot, G. & Poljak, R. J. (1987). Antigen specificity and cross-reactivity of monoclonal anti-lysozyme antibodies. *Mol. Immunol.* 24, 97–108.

Hieter, P. A., Maizel, J. V., Jr & Leder, P. (1982). Evolution of human immunoglobulin κ J region genes. *J. Biol. Chem.* 257, 1516–1522.

Imoto, T., Johnson, L. N., North, A. C. T., Phillips, D. C. & Rupley, J. A. (1972*a*). Vertebrate lysozymes. In *The Enzymes*, 3rd edit., vol. 7, pp. 665–868, Academic Press, New York.

Imoto, T., Forster, L. S., Rupley, J. A. & Tanaka, F. (1972*b*). Fluorescence of lysozyme: emissions from tryptophan residues 62 and 108 and energy migration. *Proc. Nat. Acad. Sci., U.S.A.* 69, 1151–1155.

Ish-Horowicz, D. & Burke, J. F. (1981). Rapid and efficient cosmid cloning. *Nucl. Acids Res.* 9, 2989–2998.

Jones, P. T., Dear, P. H., Foote, J., Neuberger, M. S. & Winter, G. (1986) Replacing the complementarity-determining regions of a human antibody with those from a mouse. *Nature (London)*, 321, 522–524.

Kabat, E. A. & Wu, T. T. (1971). Attempts to locate complementarity determining residues in the variable positions of light and heavy chains. *Ann. N.Y. Acad. Sci.* 190, 382–393.

Kabat, E. A., Wu, T. T., Reid-Miller, M., Perry, H. M. & Gottesman, K. S. (1987). *Sequences of Proteins of*

Immunological Interest, 4th edit., U.S. Dept of Health and Human Services, Bethesda.

Kettleborough, C. A., Saldanha, J., Heath, V. J., Morrison, C. J. & Bendig, M. M. (1991). Humanization of a mouse monoclonal antibody by CDR-grafting: the importance of framework residues on loop conformation. *Protein Engineer.* **4**, 773–783.

Kieny, M. P., Lathe, R. & Lecocq, J. P. (1983). New versatile cloning and sequencing vectors based on bacteriophage M13. *Gene*, **26**, 91–99.

Laemmli, U. K. (1970). Cleavage of structural proteins during the assembly of the head of bacteriophage T4. *Nature (London)*, **227**, 680–685.

Maeda, H., Matsushita, S., Eda, Y., Kimachi, K., Tokiyoshi, S. & Bendig, M. M. (1991). Construction of reshaped human antibodies with HIV-neutralizing activity. *Human Antibodies and Hybridomas*, **2**, 124–134.

Mathisson, P. W., Cobbold, S. P., Hale, G., Clark, M. R., Oliveira, D. B. G., Lockwood, C. M. & Waldmann, H. (1990). Monoclonal-antibody therapy in systemic vasculitis. *New Engl. J. Med.* **323**, 250–254.

Mulligan, R. C. & Berg, P. (1980). Expression of a bacterial gene in mammalian cells. *Science*, **209**, 1422–1427.

Neuberger, M. S. (1983). Expression and regulation of immunoglobulin heavy chain gene transfected into lymphoid cells. *EMBO J.* **2**, 1373–1378.

Neuberger, M. S., Williams, G. T., Mitchell, E. B., Jouhal, S. S., Flanagan, J. G. & Rabbitts, T. H. (1985). A hapten-specific chimaeric IgE antibody with human physiological effector functions. *Nature (London)*, **314**, 268–270.

Novotny, J., Bruccoleri, R. E. & Haber, E. (1990). Computer analysis of mutations that affect antibody specificity. *Proteins: Struct. Funct. Genet.* **7**, 93–98.

Orlandi, R., Güssow, D. H., Jones, P. T. & Winter, G. (1989). Cloning immunoglobulin variable domains for expression by the polymerase chain reaction. *Proc. Nat. Acad. Sci., U.S.A.* **86**, 3833–3837.

Padlan, E. A. (1991). A possible procedure for reducing the immunogenicity of antibody variable domains while preserving their ligand-binding properties. *Mol. Immunol.* **28**, 489–498.

Palm, W. & Hilschmann, N. (1973). Die primärstruktur einer kristallinen monoklonalen immunoglobulin-L-kette vom κ-Typ, subgruppe I (Bence-Jones-Protein Rei.): ein beitrag zur aufklärung der dreidimensionalen struktur der immunoglobuline. *Hoppe-Seyler's Z. Physiol. Chem.* **354**, 1651–1654.

Panka, D. J., Mudgett-Hunter, M., Parks, D. R., Peterson, L. L., Herzenberg, L. A., Haber, E. & Margolies, M. N. (1986). Variable region framework differences result in decreased or increased affinity of variant anti-digoxin antibodies. *Proc. Nat. Acad. Sci., U.S.A.* **85**, 3080–3084.

Pascual, V. & Capra, J. D. (1991). Human immunoglobulin heavy-chain variable region genes: organization, polymorphism, and expression. *Advan. Immunol.* **49**, 1–74.

Poljak, R. J., Amzel, L. M., Avey, H. P., Chen, B. L., Phizackerly, R. P. & Saul, F. (1973). Three-dimensional structure of the Fab' fragment of a human immunoglobulin at 2·8 Å resolution. *Proc. Nat. Acad. Sci., U.S.A.* **70**, 3305–3310.

Potter, H., Weir, L. & Leder, P. (1984). Enhancer-dependent expression of human κ immunoglobulin genes introduced into mouse pre-B lymphocytes by electroporation. *Proc. Nat. Acad. Sci., U.S.A.* **81**, 7161–7165.

Queen, C., Schneider, W. P., Selick, H. E., Payne, P. W., Ladolfi, N. F., Duncan, J. F., Avdalovic, N. M., Levitt, M., Junghans, R. P. & Waldmann, T. A. (1989). A humanized antibody that binds to the interleukin 2 receptor. *Proc. Nat. Acad. Sci., U.S.A.* **86**, 10029–10033.

Riechmann, L., Clark, M., Waldmann, H. & Winter, G. (1988). Reshaping human antibodies for therapy. *Nature (London)*, **332**, 323–327.

Schiffer, M., Girling, R. L., Ely, K. R. & Edmundson, A. B. (1973). Structure of a λ-type Bence-Jones protein at 3·5 Å resolution. *Biochemistry*, **12**, 4620–4631.

Schlessinger, D. H., Goldstein, G. & Niall, H. D. (1975). The complete amino acid sequence of ubiquitin, an adenylate cyclase stimulating polypeptide probably universal in living cells. *Biochemistry*, **14**, 2214–2218.

Segal, D. M., Padlan, E. A., Cohen, G. H., Rudikoff, S., Potter, M. & Davies, D. R. (1974). The three-dimensional structure of a phosphorylcholine-binding mouse immunoglobulin Fab and the nature of the antigen binding site. *Proc. Nat. Acad. Sci., U.S.A.* **71**, 4298–4302.

Segal, I. H. (1975). In *Enzyme Kinetics*, pp. 864–865, Wiley-Interscience, New York.

Takahashi, N., Ueda, S., Obata, M., Nikaido, T., Nakai, S. & Honjo, T. (1982). Structure of human immunoglobulin gamma genes: implications for evolution of a gene family. *Cell*, **29**, 671–679.

Tempest, P. R., Bremner, P., Lambert, M., Taylor, G., Furze, J. M., Carr, F. J. & Harris, W. J. (1991). Reshaping a human monoclonal antibody to inhibit human respiratory syncytial virus infection in vivo. *BioJTechnology*, **9**, 266–271.

Tramontano, A., Chothia, C. & Lesk, A. M. (1990). Framework residue 71 is a major determinant of the position and conformation of the second hypervariable region in the V_H domains of immunoglobulins. *J. Mol. Biol.* **215**, 175–182.

Tulip, W. R., Varghese, J. N., Webster, R. G., Air, G. M., Laver, W. G. & Colman, P. M. (1989). Crystal structures of neuraminidase-antibody complexes. *Cold Spring Harbor Symp. Quant. Biol.* **54**, 257–263.

Van Duuren, B. L. (1961). Solvent effects in the fluorescence of indole and substituted indole. *J. Org. Chem.* **26**, 2954.

Verhoeyen, M., Milstein, C. M. & Winter, G. (1988). Reshaping human antibodies: grafting an antilysozyme activity. *Science*, **239**, 1534–1536.

Vieira, J. & Messing, J. (1982). The pUC plasmids, an M13 mp7-derived system for insertion mutagenesis and sequencing with synthetic universal primers. *Gene*, **19**, 259–268.

Wu, T. T. & Kabat, E. A. (1970). An analysis of the sequences of the variable regions of Bence Jones proteins and myeloma light chains and their implication for antibody complementarity. *J. Exp. Med.* **132**, 211–250.

Yanisch-Perron, C., Vieira, J. & Messing, J. (1985). Improved M13 phage cloning vectors and host strains: nucleotide sequences of the M13 mp18 and pUC19 vectors. *Gene*, **33**, 103–119.

Zoller, M. J. & Smith, M. (1982). Oligonucleotide-directed mutagenesis using M13-derived vectors: an efficient and general procedure for the production of point mutations in any fragment of DNA. *Nucl. Acids Res.* **10**, 6487–6500.

Edited by J. Karn